Modeling of Guided Waves for Detection of Linear and Nonlinear Structural Damage

Yanfeng Shen, Victor Giurgiutiu
Department of Mechanical Engineering, University of South Carolina, Columbia, SC, 29208, USA

ABSTRACT

This paper presents an analytical approach to modeling guided Lamb waves interacting with linear and nonlinear structural damage. The active sensing process using piezoelectric wafer active sensors (PWAS) was modeled in the following four steps: (1) guided waves generation by transmitter PWAS (T-PWAS); (2) Lamb wave multi-mode dispersive propagation in the host structure; (3) linear and nonlinear interaction between Lamb waves and damage; (4) guided waves detection by receiver PWAS (R-PWAS). Structural damage was modeled as a new wave source, where guided waves are transmitted, reflected, and mode-converted. In addition, when guided waves interact with nonlinear damage, nonlinear higher harmonics will also be present. Real time sensing signal at R-PWAS was obtained, as well as the time-space wave field and the frequency-wavenumber representation.

A Graphical User Interface (GUI) called WaveFormRevealer (WFR) was developed based on this analytical model. High frequency guided wave propagation in thick plates was done first. Beside fundamental modes (S0 and A0), higher wave modes were also observed. These analytical results were verified by experiments. Analytical simulation of linear interaction between Lamb waves and a notch was done next and compared with experiments. New wave packets due to mode conversion at the notch were observed. Subsequently, the nonlinear interaction between Lamb waves and a breathing crack was investigated using a contact finite element model (FEM). Distinctive nonlinear effects were noticed in both FEM simulation and analytical solutions. The paper finishes with summary, conclusions, and suggestions for future work.

Keywords: structural health monitoring, nondestructive evaluation, guided waves, Lamb waves, damage detection, piezoelectric wafer active sensors, nonlinear ultrasonics, higher harmonics

1. INTRODUCTION

Guided waves serve as good candidates for structural health monitoring systems due to their nice properties of long propagating distances and sensitivity to structural changes[1]. However, the modeling of guided waves is challenging, because they propagate in structures with multi-mode dispersive characteristics[2]. Moreover, when guided waves interact with damage, they will be transmitted, reflected, scattered and mode converted. Nonlinear interaction with damage may also exist and this will introduce distinctive features like nonlinear higher harmonics[3, 4]. To solve such complicated problems, numerical methods like finite element method (FEM) and boundary element method (BEM) are usually adopted. However, to ensure the accuracy of simulating high-frequency waves of short wavelengths, the transient analysis requires considerably small time step and very fine mesh ($T/\Delta t$, $\lambda/l_{FEM} \geq 20 \sim 30$), which is expensive both in computational time and computer resources[5, 6]. The design of a SHM system requires computationally-efficient predictive tools that permit the exploration of a wide parameter space to identify the optimal combination between the transducers type, size, number and guided wave characteristics (mode type, frequency, and wavelength) to achieve best detection and quantification of a certain damage type. Such parameter space exploration desiderate can be best achieved with analytical tools which are fast and efficient.

PWAS transducers are a convenient way of transmitting and receiving guided waves in structures for SHM applications[7]. The analytical model of PWAS generated Lamb waves and its tuning effect has been investigated, and the exact solution of multi-modal guided Lamb waves generated by PWAS transducers is derived in Ref. 8. Extension of tuning concepts to 2-D analytical models of Lamb waves generated by finite-dimensional piezoelectric transducers was given in Ref. 9. These analytical developments facilitate the understanding of PWAS-coupled Lamb waves for SHM applications. However, these analytical solutions only applied to guided wave propagation in pristine structures, whereas the use of Lamb waves in SHM applications requires that their interaction with damage be also studied. After interacting with damage, Lamb waves will carry damage information resulting in waveforms with special characteristics (phase change,

new wave packets generation through mode conversion, higher-harmonic components, etc.), which need to be investigated for damage detection.

In this paper, we describe an analytical approach based on the 1D (straight crested) guided wave propagation analysis. In our study, we inserted the damage effect into the analytical model by considering wave transmission, reflection, mode conversion, and higher harmonics components described through damage interaction coefficients at the damage site. We do not attempt to derive these damage interaction coefficients here, but assume that they are available either from literature or from FEM, BEM analysis performed in a separate computational module. This analytical procedure was coded into MATLAB and the WaveFormRevealer (WFR) graphical user interface (GUI) was developed. The WFR can generate fast predictions of waveforms resulting from Lamb waves' interaction with damage for arbitrary positioning of PWAS transmitters and receivers with respect to damage and with respect to each other.

2. PWAS PRINCIPLES

Piezoelectric wafer active sensors (PWAS) couple the electrical and mechanical effects (mechanical strain, S_{ij}, mechanical stress, T_{kl}, electrical field, E_k, and electrical displacement, D_j) through the tensorial piezoelectric constitutive equations

$$\begin{aligned} S_{ij} &= s^E_{ijkl} T_{kl} + d_{kij} E_k \\ D_j &= d_{kij} T_{kl} + \varepsilon^T_{jk} E_k \end{aligned} \tag{1}$$

where is the mechanical compliance of the material measured at zero electric field ($E = 0$), ε^T_{jk} is the dielectric permittivity measured at zero mechanical stress ($T = 0$), and d_{kij} represents the piezoelectric coupling effect. PWAS utilize the d_{31} coupling between in-plane strains, S_1, S_2 and transverse electric field E_3.

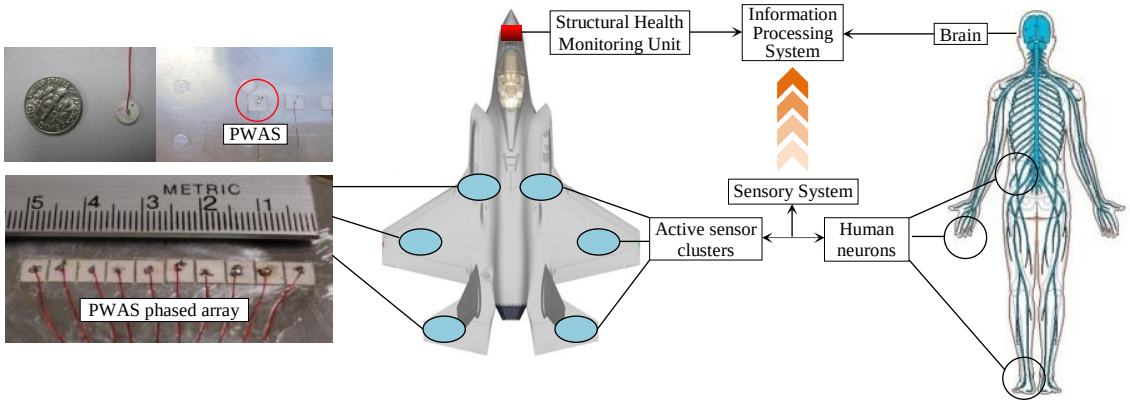

Figure 1: Piezoelectric wafer active sensors and their applications in SHM to achieve structural self-awareness (adapted after Ref. 10)

Compared with conventional ultrasonic transducers, PWAS are small, lightweight, low cost, unobtrusive, and invasive to structures. They can be permanently bonded on host structures and achieve real time sensing and in-situ monitoring. PWAS transducers can be used as both transmitters and receivers, which enable active sensing SHM of the structures and achieve structural self-awareness (Figure 1).

PWAS can serve several purposes[7]: (a) high-bandwidth strain sensors; (b) high-bandwidth wave exciters and receivers; (c) resonators; (d) embedded modal sensors with the electromechanical (E/M) impedance method. By application types, PWAS transducers can be used for (i) active sensing of far-field damage using pulse-echo, pitch-catch, and phased-array methods, (ii) active sensing of near field damage using high-frequency E/M impedance method and thickness gage mode, and (iii) passive sensing of damage-generating events through detection of low-velocity impacts and acoustic emission at the tip of advancing cracks.

3. ANALYTICAL MODELING OF GUIDED WAVES INTERACTION WITH DAMAGE

Figure 2 shows the pitch-catch active sensing method for damage detection: the T-PWAS transducer generates ultrasonic guided waves which propagate into the structure, interact with structural damage at $x = x_d$, carry the damage information with them, and are picked up by the R-PWAS transducer at $x = x_r$.

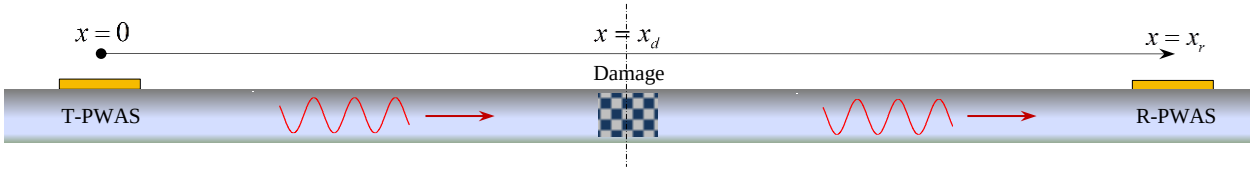

Figure 2: A pitch-catch configuration between a transmitter PWAS and a receiver PWAS

The analytical model is constructed in frequency domain shown in the flow chart (Figure 3), and can be illustrated in the following nine steps:

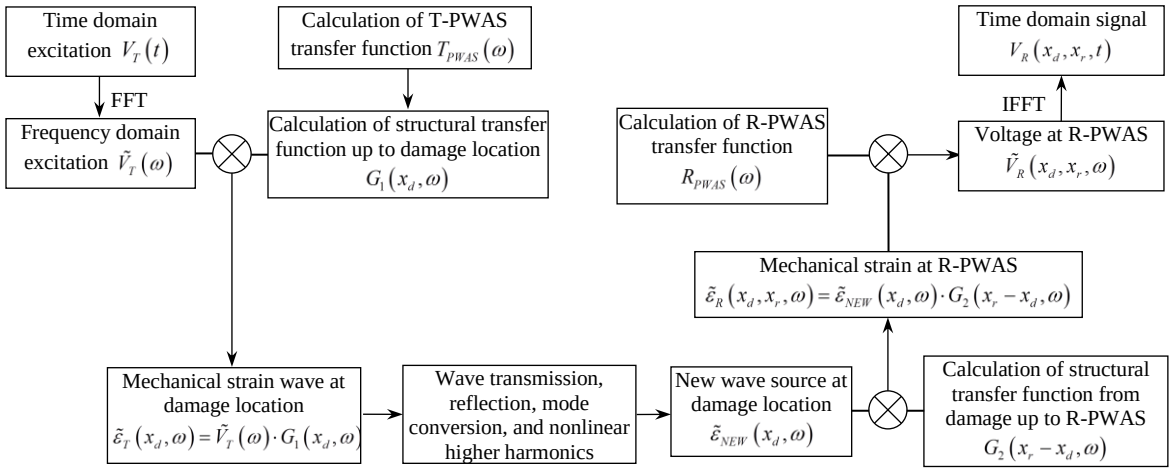

Figure 3: Flow chart for guided wave propagation and interaction with damage

STEP 1: Perform Fourier transform of the time-domain excitation signal $V_T(t)$ to obtain the frequency domain excitation spectrum, $\tilde{V}_T(\omega)$.

STEP 2: Calculate the T-PWAS transfer function, which describes electrical to mechanical transduction. This transfer function is given in Ref. 11

$$T_{PWAS}(\omega) = \frac{d_{31}}{\mu s_{11}^E}\frac{r(\omega)}{1-r(\omega)} \tag{2}$$

where d_{31} is the piezoelectric coefficient, s_{11}^E is the mechanical compliance of PWAS, Lame's constant μ represents the shear modulus of the host structure, and $r(\omega)$ denotes the frequency-dependent stiffness ratio:

$$r(\omega) = \frac{k_{str}(\omega)}{k_{PWAS}} \tag{3}$$

where

$$k_{PWAS} = \frac{h_{PWAS}}{s_{11}^E a}, \quad k_{str}(\omega) = -\mu\left\{\sum_n \frac{N_S(\xi_{S_n})}{D_S'(\xi_{S_n})}\frac{\sin\xi_{S_n}a}{\xi_{S_n}}e^{i\xi_{S_n}a} + \sum_n \frac{N_A(\xi_{A_n})}{D_A'(\xi_{A_n})}\frac{\sin\xi_{A_n}a}{\xi_{A_n}}e^{i\xi_{A_n}a}\right\}^{-1} \tag{4}$$

$$N_s(\xi)=\xi\beta\left(\xi^2+\beta^2\right)\cos\alpha d\cos\beta d;\quad D_s=\left(\xi^2-\beta^2\right)^2\cos\alpha d\sin\beta d+4\xi^2\alpha\beta\sin\alpha d\cos\beta d$$
$$N_A(\xi)=\xi\beta\left(\xi^2+\beta^2\right)\sin\alpha d\sin\beta d;\quad D_A=\left(\xi^2-\beta^2\right)^2\sin\alpha d\cos\beta d+4\xi^2\alpha\beta\cos\alpha d\sin\beta d \tag{5}$$
$$\alpha^2=\frac{\omega^2}{c_p^2}-\xi^2;\quad \beta^2=\frac{\omega^2}{c_s^2}-\xi^2;\quad c_p=\sqrt{\frac{\lambda+2\mu}{\rho}};\quad c_s=\sqrt{\frac{\mu}{\rho}};$$

h_{PWAS} and a are the thickness and half the length of T-PWAS, λ denotes Lame's constants of the structural material; ρ is the material density. ξ represents the wavenumber of a specific mode for certain frequency ω, calculated from Rayleigh-Lamb equation:

$$\frac{\tan\beta d}{\tan\alpha d}=\left[\frac{-4\alpha\beta\xi^2}{\left(\xi^2-\beta^2\right)^2}\right]^{\pm1} \tag{6}$$

where +1 exponent corresponds to symmetric Lamb wave modes and -1 exponent corresponds to antisymmetric Lamb wave modes.

STEP 3: Calculate the frequency-domain structural transfer function up to the damage location, $G_1(x_d,\omega)$ based on the exact solution of multimodal guided Lamb waves generated by PWAS transducers. The structure transfer function $G_1(x_d,\omega)$ is given by Eq. (99) of Ref. 7, page 327, which gives the in-plane wave strain at the plate surface as

$$\varepsilon_x(x,t)=-i\frac{a\tau_0}{\mu}\left\{\sum_{\xi^S}(\sin\xi^S a)\frac{N_S\left(\xi^S\right)}{D_S^{'}\left(\xi^S\right)}e^{-i\left(\xi^S x-\omega t\right)}+\sum_{\xi^A}(\sin\xi^A a)\frac{N_A\left(\xi^A\right)}{D_A^{'}\left(\xi^A\right)}e^{-i\left(\xi^A x-\omega t\right)}\right\} \tag{7}$$

In Eq (7), the transduction coefficient $-i\frac{a\tau_0}{\mu}$ converts the shear stress applied by PWAS into wave strain in the structure. In this paper, we further studied the electrical to mechanical transduction at T-PWAS, and this term is replaced by $T_{PWAS}(\omega)$ which converts applied voltage to in plane strain. If only the two fundamental modes, S0 and A0, are present, then $G_1(x_d,\omega)$ can be written as

$$G_1(x_d,\omega)=S(\omega)e^{-i\xi^S x_d}+A(\omega)e^{-i\xi^A x_d} \tag{8}$$
$$S(\omega)=T_{PWAS}(\omega)\sin\xi^S a\,\frac{N_S\left(\xi^S\right)}{D_S^{'}\left(\xi^S\right)},\quad A(\omega)=T_{PWAS}(\omega)\sin\xi^A a\,\frac{N_A\left(\xi^A\right)}{D_A^{'}\left(\xi^A\right)} \tag{9}$$

The modal participation functions $S(\omega)$ and $A(\omega)$ determine the amplitudes of the S0 and A0 wave modes. The terms $\sin(\xi^S a)$ and $\sin(\xi^A a)$ control the tuning between Lamb waves and the T-PWAS transducer.

STEP 4: Multiply the structural transfer function by frequency-domain excitation signal to obtain the frequency domain strain waves at the R-PWAS, i.e., $\tilde{\varepsilon}_D(x_d,\omega)=G_1(x_d,\omega)\cdot\tilde{V}_T(\omega)$. This signal could be decomposed into symmetric and antisymmetric components

$$\tilde{\varepsilon}_D^S(x_d,\omega)=S(\omega)\tilde{V}_T(\omega)e^{-i\xi^S x_d} \tag{10}$$
$$\tilde{\varepsilon}_D^A(x_d,\omega)=A(\omega)\tilde{V}_T(\omega)e^{-i\xi^A x_d} \tag{11}$$

STEP 5: The waves at the damage location take the damage information by considering transmission, reflection, mode conversion, and nonlinear higher harmonics. Each of these addition phenomena is modeled as a new wave source at the damage location using damage interaction coefficients (Figure 4). We distinguish two damage interaction types: (a) linear, and (b) nonlinear, as discussed next.

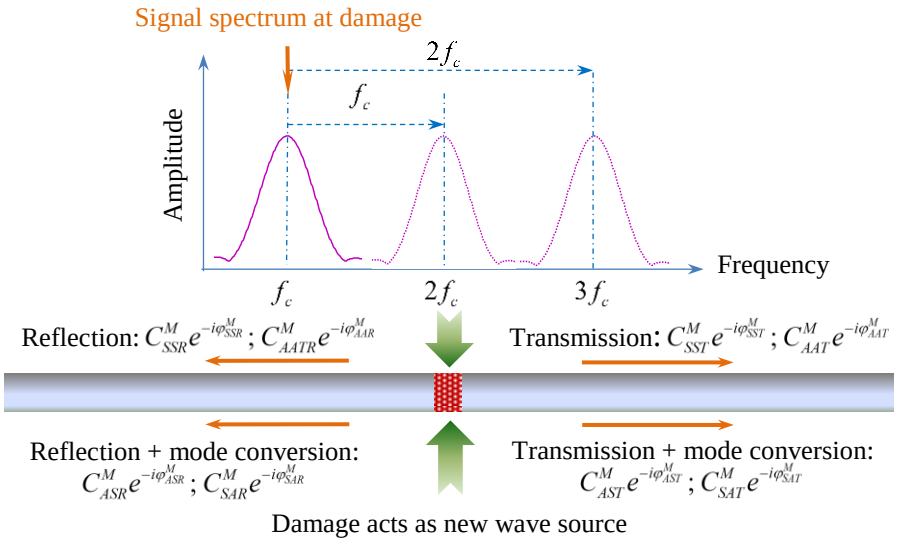

Figure 4: Modeling wave transmission, reflection, mode conversion, higher harmonics components.

(a) Linear damage interaction

For 1-D model, the most general case of linear interaction between guided waves and damage will involve wave transmission, reflection, and mode conversion. The modeling of such phenomena is realized by using complex-amplitude damage interaction coefficients. Our notations are as follows: we use three letters to describe the interaction phenomena, with the first letter denoting the incident wave mode, the second letter representing the resulting wave mode, and the third letter meaning the propagation direction (transmission/reflection). For instance, SST (symmetric-symmetric-transmission) means the incident symmetric waves transmitted as symmetric waves, while SAT (symmetric-antisymmetric-transmission) means incident symmetric waves transmitted and mode converted to antisymmetric waves. Thus the complex-amplitude damage interaction coefficient $C_{SST}\cdot e^{-i\varphi_{SST}}$ denotes the incident symmetric mode transmitted as symmetric mode with magnitude C_{SST} and phase φ_{SST}. Similarly, $C_{SAT}\cdot e^{-i\varphi_{SAT}}$ represents the symmetric mode transmitted and mode converted to antisymmetric mode with magnitude C_{SAT} and phase φ_{SAT}. These coefficients are determined by the features (type and geometry) of the damage and are to be imported into the analytical model.

(b) Nonlinear damage interaction

The center frequency of waves arriving at the damage location can be obtained from Eq. (10) or (11) as ω_c. The 2nd and 3rd higher harmonics act as wave sources with center frequencies of $2\omega_c$ and $3\omega_c$ respectively. Modeling of higher harmonics is achieved by moving the frequency domain signal at the damage location to the right hand side of the frequency axis by ω_c and $2\omega_c$, i.e., $\tilde{\varepsilon}_{2D}(x_d,\omega)=\tilde{\varepsilon}_D(x_d,\omega-\omega_c)$ and $\tilde{\varepsilon}_{3D}(x_d,\omega)=\tilde{\varepsilon}_D(x_d,\omega-2\omega_c)$ represent the 2nd and 3rd higher harmonics nonlinear wave source.

The nonlinear damage interaction coefficients are defined in the same way as the linear ones. For instance, the complex-amplitude damage interaction coefficient $C^M_{SST}\cdot e^{-i\varphi^M_{SST}}$ denotes the *M*th nonlinear higher harmonics generated from symmetric incident waves and transmitted as symmetric mode waves with magnitude C^M_{SST} and phase φ^M_{SST}.

STEP 6: The guided waves from the new wave sources created at the damage location propagate through the rest of the structure and arrive at the R-PWAS. The mechanical strain at R-PWAS is calculated in frequency domain as

$$\tilde{\varepsilon}_R\left(x_d, x_r, \omega\right) = \sum_{M=1}^{m}\left[C_{SST}^{M} e^{-i\varphi_{SST}^{M}} \cdot \tilde{\varepsilon}_{MD}^{S}\left(x_d, \omega\right) + C_{AST}^{M} e^{-i\varphi_{AST}^{M}} \cdot \tilde{\varepsilon}_{MD}^{A}\left(x_d, \omega\right)\right] e^{-i\xi^{S}\left(x_r - x_d\right)} + \sum_{M=1}^{m}\left[C_{AAT}^{M} e^{-i\varphi_{AAT}^{M}} \cdot \tilde{\varepsilon}_{MD}^{A}\left(x_d, \omega\right) + C_{SAT}^{M} e^{-i\varphi_{SAT}^{M}} \cdot \tilde{\varepsilon}_{MD}^{S}\left(x_d, \omega\right)\right] e^{-i\xi^{A}\left(x_r - x_d\right)} \tag{12}$$

where M is the number of higher harmonics considered. For linear interaction with damage, M equals to one.

STEP 7: Calculate R-PWAS transfer function, which describes mechanical to electrical transduction. This transfer function is derived from the piezoelectric sensing equation[7]

$$E_i = g_{ikl} T_{kl} + \beta_{ik}{}^{T} D_k + \tilde{E}_i \theta \tag{13}$$

The coefficient g_{ikl} is the piezoelectric voltage coefficient and represents how much electric field is induced per unit stress. The coefficient $\tilde{E}_i$ is the pyroelectric voltage coefficient and represents how much electric field is induced per unit temperature change. The final solution of electric voltage transduced from mechanical strain takes the following form[11, 12]:

$$R(\omega) = \frac{g_{31} h_{PWAS}}{2 a_R s_{11}^{E}} \int_{-a_R}^{a_R} e^{-i\xi x} dx = \frac{g_{31} h_{PWAS}}{a_R s_{11}^{E}} \frac{\sin\left(\xi a_R\right)}{\xi} \tag{14}$$

where h_{PWAS} and a_R are the thickness and half the length of R-PWAS. g_{31} denotes the piezoelectric voltage coefficient mentioned in Eq (13).

STEP 8: Multiply the mechanical strain at the sensing location with the transduction function of R-PWAS to obtain the electric voltage converted back from mechanical strain wave. The sensing signal in frequency domain is calculated as

$$\begin{aligned}\tilde{V}_R\left(x_d, x_r, \omega\right) &= \tilde{\varepsilon}_R\left(x_d, x_r, \omega\right) \cdot R(\omega) \\ &= \sum_{M=1}^{m}\left[C_{SST}^{M} e^{-i\varphi_{SST}^{M}} \cdot \tilde{\varepsilon}_{MD}^{S}\left(x_d, \omega\right) + C_{AST}^{M} e^{-i\varphi_{AST}^{M}} \cdot \tilde{\varepsilon}_{MD}^{A}\left(x_d, \omega\right)\right] e^{-i\xi^{S}\left(x_r - x_d\right)} \cdot R^{S}\left(\omega\right) \\ &+ \sum_{M=1}^{m}\left[C_{AAT}^{M} e^{-i\varphi_{AAT}^{M}} \cdot \tilde{\varepsilon}_{MD}^{A}\left(x_d, \omega\right) + C_{SAT}^{M} e^{-i\varphi_{SAT}^{M}} \cdot \tilde{\varepsilon}_{MD}^{S}\left(x_d, \omega\right)\right] e^{-i\xi^{A}\left(x_r - x_d\right)} \cdot R^{A}\left(\omega\right)\end{aligned} \tag{15}$$

where $R^{S}\left(\omega\right)$ and $R^{A}\left(\omega\right)$ denote the R-PWAS transfer function for symmetric and antisymmetric modes respectively.

STEP 9: Perform inverse Fourier transform to obtain the time domain signal at R-PWAS

$$V_R(x_d, x_r, t) = IFFT\{\tilde{V}_R(x_d, x_r, \omega)\} \tag{16}$$

It should be noted that the above analysis only considers S0 and A0 modes. But the principle could be easily extended to higher modes (S1, A1, etc.). The difficulty with extending to higher modes will be on defining the increasing number of transmission, reflection, mode conversion coefficients. For each excited Lamb mode, the interaction with damage may result in more mode conversion possibilities.

4. ANALYTICAL SIMULATION TOOL DEVELOPMENT – WAVEFORMREVEALER

The analytical representation was coded in MATLAB and resulted in the graphical user interface (GUI) called WaveFormRevealer (WFR). WFR is an analytical simulation tool that allows users to control several parameters: structure material properties, PWAS properties, location of sensors, location of damage, damage type (linear/nonlinear damage of various severities), and excitation signal (frequencies, count numbers, signal mode excitation, arbitrary waveform type, etc.). Figure 5 shows the WaveFormRevealer interfaces.

The **main interface** calculates the real time sensing signals at two R-PWAS transducers located at different positions along the wave propagation path (shown in Figure 5a). It also allows users to obtain the dispersion curve, tuning curve, frequency component of S0 and A0 waves, and structure transfer function. The **damage information platform** allows users to input linear and nonlinear damage interaction coefficients (Figure 5b). The **PWAS module** allows users to define T-PWAS and R-PWAS geometric and material properties (Figure 5c). The **guided wave spatial propagation solver** is like a B-scan, which calculates the time-space domain wave field. Thus the spatial waveform can be obtained at

any instance during wave propagation (Figure 5d). The spatial propagation solver can also conduct frequency-wavenumber analysis[13] to see the wave mode components of the signal (Figure 5e). With this analytical tool, considerable computation efficiency for large parameter space exploration can be achieved. It may take several hours for commercial finite element software to obtain an acceptable-accuracy solution for high frequency, long distance propagating waves; but it takes only several seconds to obtain the same solution with the WFR. The WFR is available at: http://www.me.sc.edu/Research/lamss/html/software.html

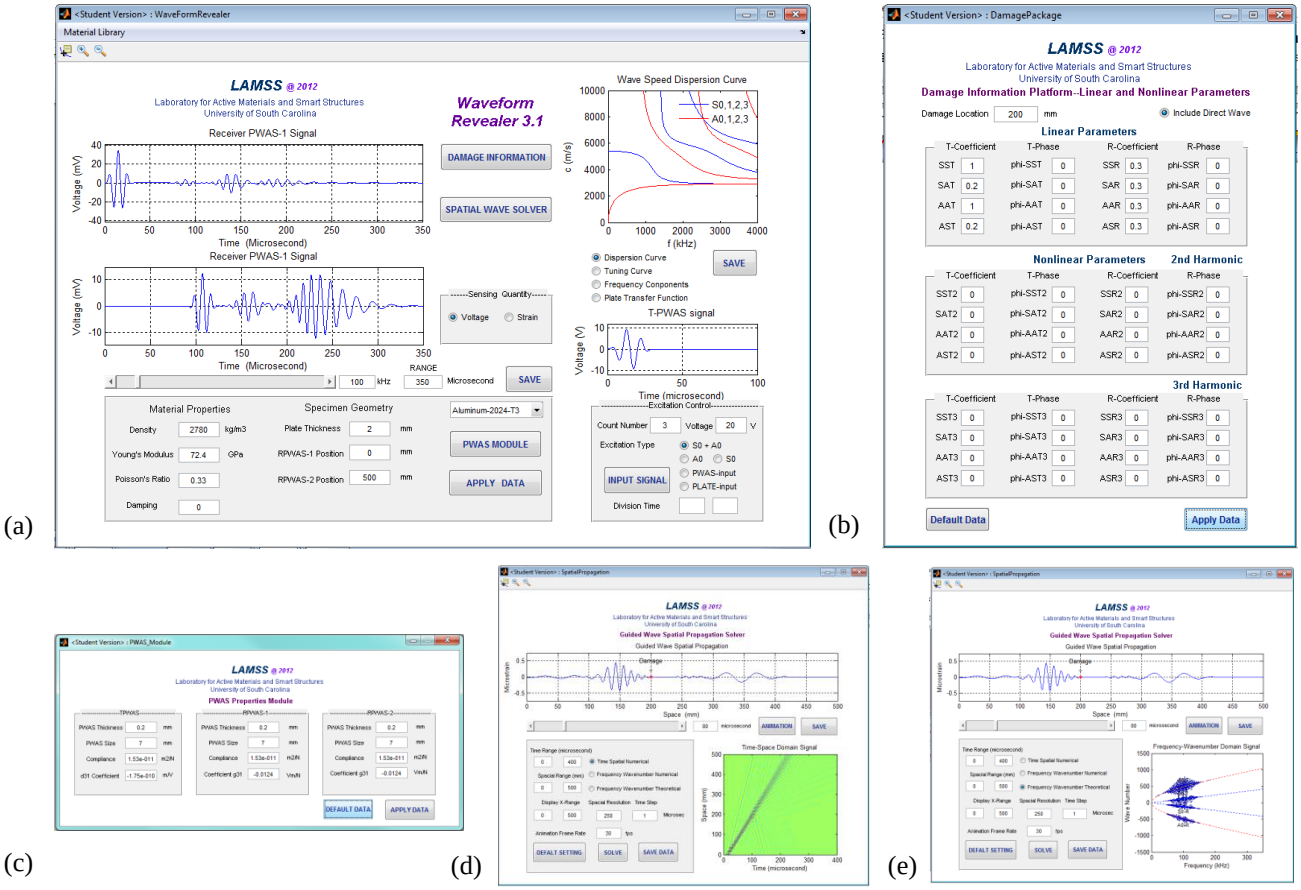

Figure 5: GUI of WFR: (a) main interface; (b) damage information platform; (c) PWAS module; (d) spatial propagation solver with time-space domain signal; (e) spatial propagation solver with frequency-wavenumber analysis

5. EXPERIMENTAL VERIFICATIONS

5.1 Multimodal guided wave propagation in a pristine structure

Figure 6 shows the experiment setup. A pitch-catch active sensing experiment was conducted on a pristine 3.17-mm thick aluminum 7075-T6 plate. The transmitter PWAS (T-PWAS) sends out ultrasonic guided waves into the structure. The guided waves i.e., Lamb waves propagate in the plate, undergoing dispersion, and are picked up by the receiver PWAS (R-PWAS). The Lamb waves are multimodal; hence several wave packets appear in the received signal. The final waveform has the contribution from all the propagating modes. Agilent 33120A Arbitrary Waveform Generator is used to generate 3-count Hanning window modulated tone burst excitations. A Tektronix Digital Oscilloscope is used to record the experimental waveforms.

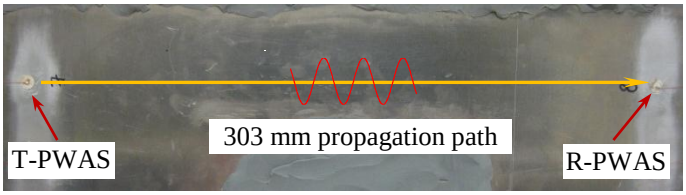

Figure 6: Experiment setup for multi-mode Lamb wave propagation

Figure 7 shows the comparison between the analytical solution and experiments for 300 kHz and 600 kHz cases. It can be observed that at 300 kHz, only S0 and A0 modes exist. The analytical solution matches well with experimental data. At 600 kHz, S0, A0, and A1 modes exist simultaneously. The simulation results and the experimental data have slight differences. This may be due to the fact that 1-D analytical formulas are used in this study. The actual wave propagation in the experimental specimen was subject to 2-D geometric spreading, which modified the wave amplitude.

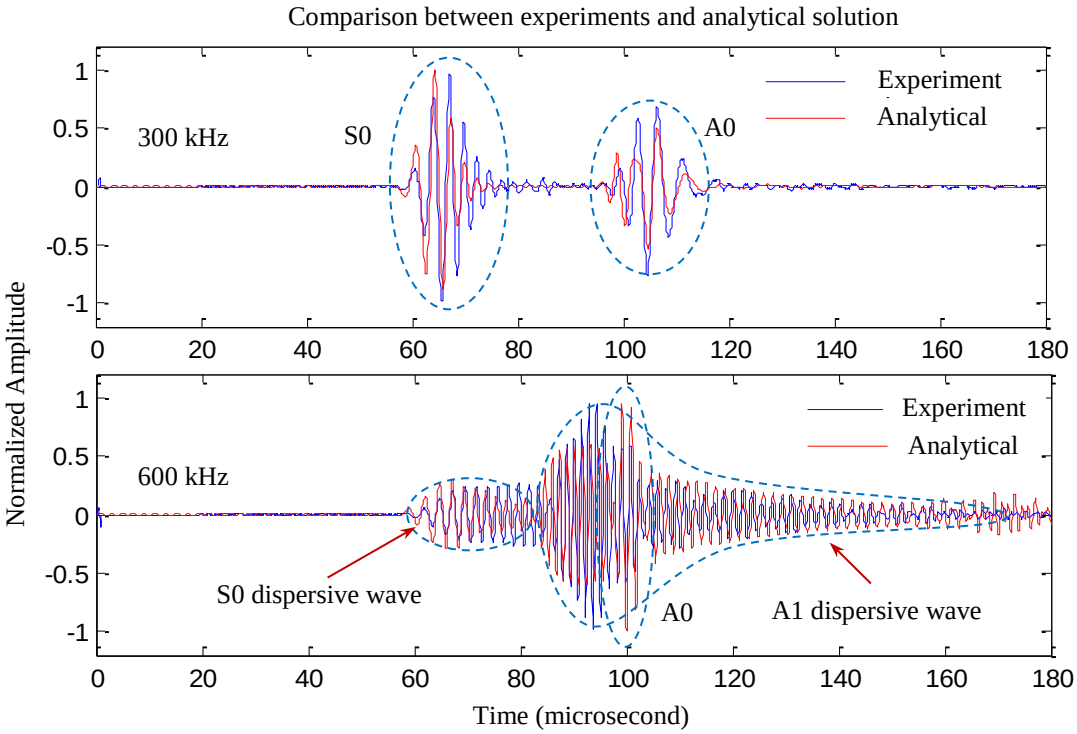

Figure 7: Comparison between analytical solution and experiment for multi-mode Lamb wave propagation in a pristine 3.17-mm aluminum plate

5.2 Linear interaction between guided waves and damage

Figure 8 shows the experiment for studying the linear interaction between guided Lamb waves and damage. Three PWAS transducers were used, one as the transmitter, and the other two as receivers. A notch was machined between T-PWAS and R-PWAS1. The Lamb waves generated by T-PWAS propagate along the structure, interact with the notch. The waves were transmitted, reflected and mode converted at the notch. The transmitted waves were picked up by R-PWAS1, and the reflected waves were picked up by R-PWAS2. T-PWAS and R-PWAS1 work in pitch-catch active sensing mode, while T-PWAS and R-PWAS2 work in pulse-echo active sensing mode. The damage interaction coefficients are physically determined by the size, severity, type of the damage. In this study, we used a trial-and-error approach to tune the damage interaction coefficients to the data obtained from the experiments.

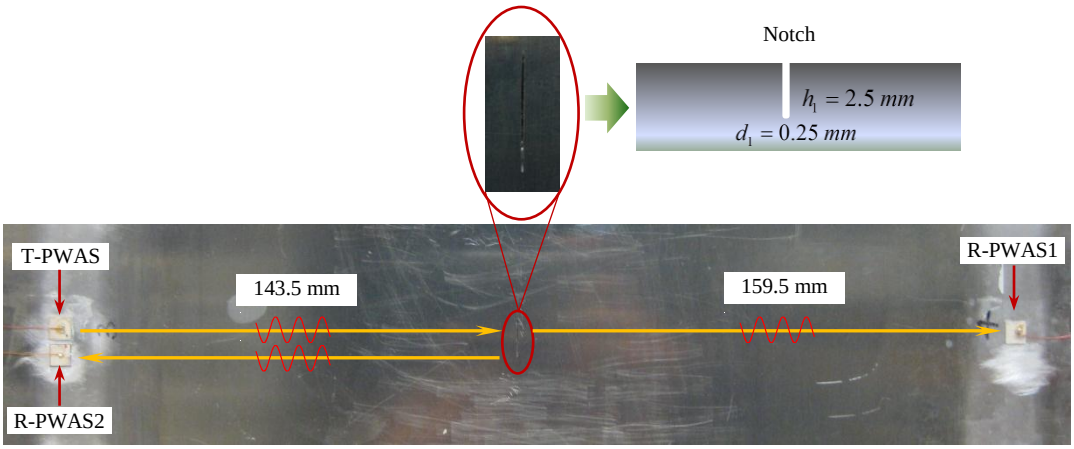

Figure 8: Experiment for linear interaction between guided Lamb waves and a notch

5.2.1 Pitch-catch mode

The adjusted damage interaction coefficients which gave best match with experiments for 150 kHz excitation case are shown in Table 1. It should be noted the interaction coefficients are frequency-dependent, and vary for each excitation frequency.

Table 1: Damage interaction coefficients for pitch-catch mode

Magnitude Coefficient	C^1_{SST}	C^1_{SAT}	C^1_{AAT}	C^1_{AST}
Value (normalized)	0.55	0.11	0.8	0.06
Phase Coefficient	φ^1_{SST}	φ^1_{SAT}	φ^1_{AAT}	φ^1_{AST}
Value (degree)	-30	30	0	30

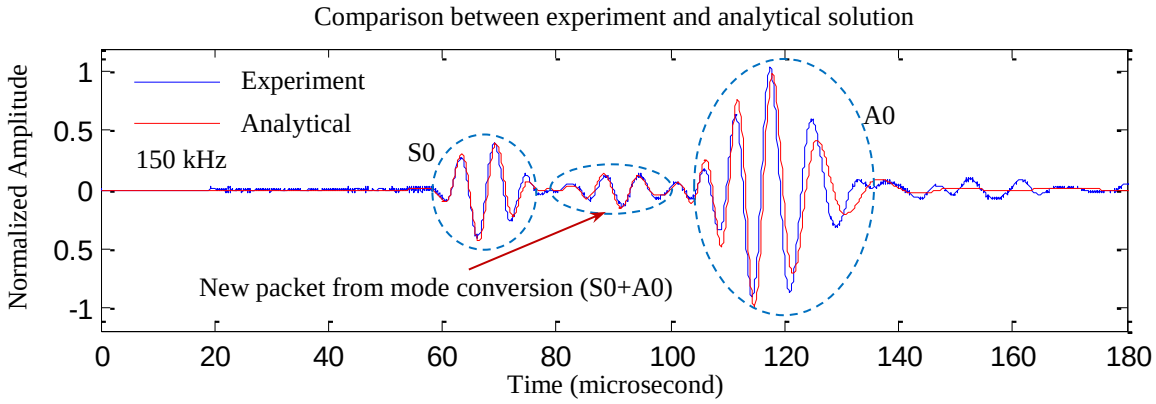

Figure 9: Linear interaction between Lamb waves and a notch (pitch-catch mode)

Figure 9 shows the comparison between experiment and analytical solution. It could be observed that the analytical solution and the experimental data match well with each other. It can be noticed that beside the fundamental S0 and A0 wave packets, a new packet appears due to the mode conversion at the notch. During the interaction, S0 waves will be mode converted to A0 waves traveling slower than the S0 wave packet and left behind. A0 waves will be mode converted to S0 waves traveling faster, leading the way and escaping from the A0 wave packet. The S0 and A0 waves generated from mode conversion mixed together at the receiver PWAS for this experiment, and formed the new wave packet. So the new wave packet contains both symmetric mode and antisymmetric mode waves.

5.2.2 Pulse-echo mode

For the pulse-echo mode experiment, 3-count Hanning window modulated tone burst signal with the center frequency of 95.5 kHz was used as the excitation. The adjusted damage interaction coefficients which gave best match with the experiment are shown in Table 2.

Table 2: Damage interaction coefficients for pulse-echo mode

Magnitude Coefficient	C^1_{SSR}	C^1_{SAR}	C^1_{AAR}	C^1_{ASR}
Value (normalized)	0.2	0.04	0.12	0.04
Phase Coefficient	φ^1_{SSR}	φ^1_{SAR}	φ^1_{AAR}	φ^1_{ASR}
Value (degree)	60	60	-60	60

Figure 10 shows the analytical solution compared with the experiment. The reflected S0 and A0 wave packets could be observed. The new waves between S0 and A0 wave packets are from mode conversion at the notch. The analytical simulation matches the experiment data. But differences are noticed: first, the direct waves have a phase shit due to the fact that the R-PWAS2 and T-PWAS were some distance away from each other, while in our analytical model, we considered them to be at the same location; second, the boundary reflections were present and mixed with the weak echoes from the notch in the experiment, but in our model, the boundary reflections were not considered.

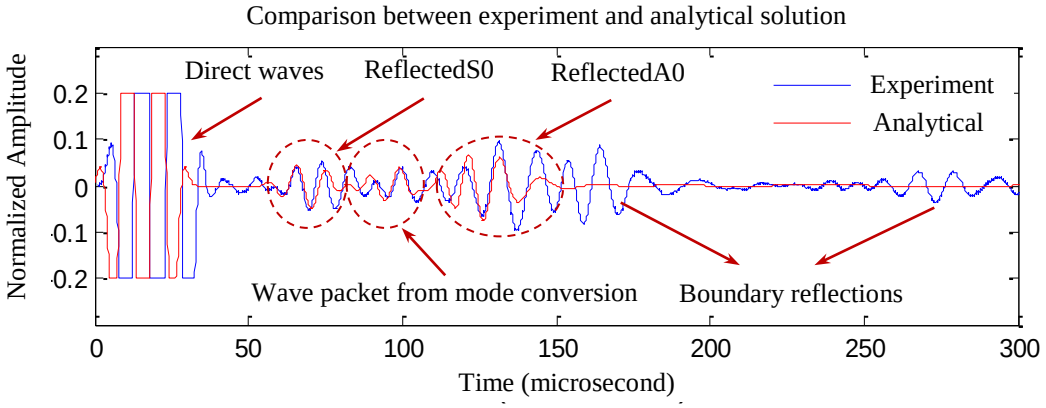

Figure 10: Linear interaction between Lamb waves and a notch (pulse-echo mode)

5.3 Nonlinear interaction between guided waves and damage

Nonlinear interaction between guided waves and damage may also exist, especially when micro fatigue cracks present in structures. These cracks may close and open under wave cycles, changing the apparent local structural stiffness, and bring nonlinearity into the interrogating waves. The nonlinear interaction with these breathing cracks will generate distinctive nonlinear higher harmonics, which could provide diagnostic information for monitoring crack severity and growth[14].

5.3.1 Finite element simulation of guided waves interaction with a nonlinear breathing crack

A nonlinear transient finite element simulation (FEM) was conducted to study how guided Lamb waves interact with a breathing crack. The PWAS transducers were modeled with coupled field elements, which couple the electrical and mechanical behaviors of piezoelectric materials. Contact elements were used to model the breathing crack. The ultrasonic waves generated by the transmitter PWAS (T-PWAS) propagate into the structure, interact with the breathing crack, acquire nonlinear features, and are picked up by the receiver PWAS (R-PWAS). The finite element model is shown in Figure 11. A 5 count tone burst signal centered at 100 kHz was used as the excitation.

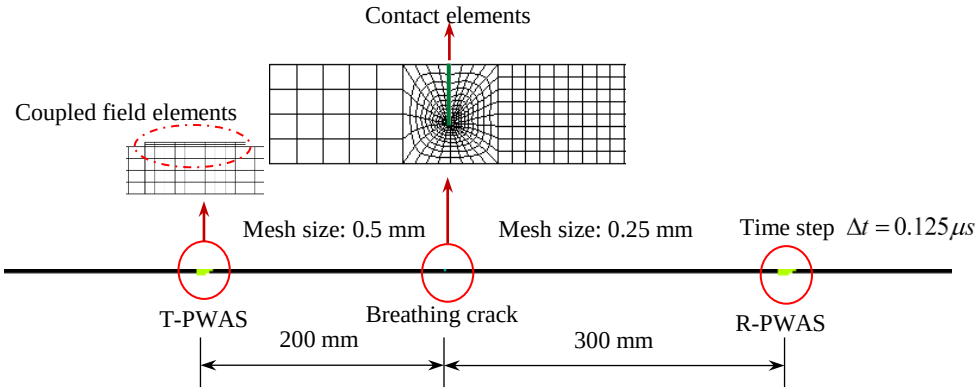

Figure 11: Finite element simulation of nonlinear interaction between Lamb waves and a breathing crack

Figure 12 shows the breathing crack open and close behavior under tension and compression wave cycles. It could be observed the breathing crack opens under tension and closes under compression for both S0 and A0 modes[15, 16].

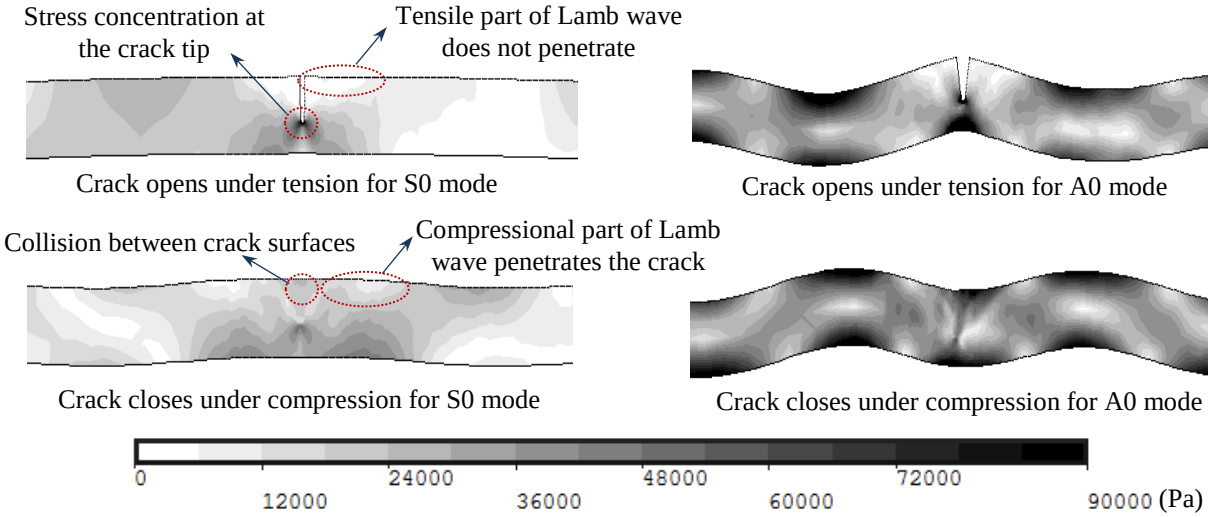

Figure 12: Breathing crack open and close under wave cycles

5.3.2 Comparison between analytical solution and FEM model

The nonlinear interaction coefficients were extracted from the FEM model and applied to the analytical model. The damage interaction coefficients are shown in Table 3.

Table 3: Nonlinear interaction coefficients

Magnitude Coefficient.	C^1_{SST}	C^1_{SAT}	C^1_{AAT}	C^1_{AST}	C^2_{SST}	C^2_{SAT}	C^2_{AAT}	C^2_{AST}	C^3_{SST}	C^3_{SAT}	C^3_{AAT}	C^3_{AST}
Value (normalized)	0.900	0.420	0.820	0.100	0.082	0.100	0.050	0.110	0.032	0.038	0.005	0.025
Phase Coefficient	φ^1_{SST}	φ^1_{SAT}	φ^1_{AAT}	φ^1_{AST}	φ^2_{SST}	φ^2_{SAT}	φ^2_{AAT}	φ^2_{AST}	φ^3_{SST}	φ^3_{SAT}	φ^3_{AAT}	φ^3_{AST}
Value (degree)	0	100	-35	90	0	0	120	90	0	0	0	0

Figure 13 shows the comparison between FEM simulation and analytical solution. The FEM and analytical solution agree well with each other, because the nonlinear interaction coefficients are extracted from the FEM model. The time domain signal shows clear nonlinear features, with S0 waveform distorted, and obvious zigzags in the new wave packet. The frequency domain analysis shows distinctive nonlinear higher harmonics in all the wave packets. Since in our

analytical model, we only input the first three higher harmonics information, the frequency domain analysis of the analytical solution only shows the first three defined harmonics; but in the FEM simulation results, even higher harmonics components are present. However, the first three higher harmonics are already capable of rendering an acceptably accurate time domain signal.

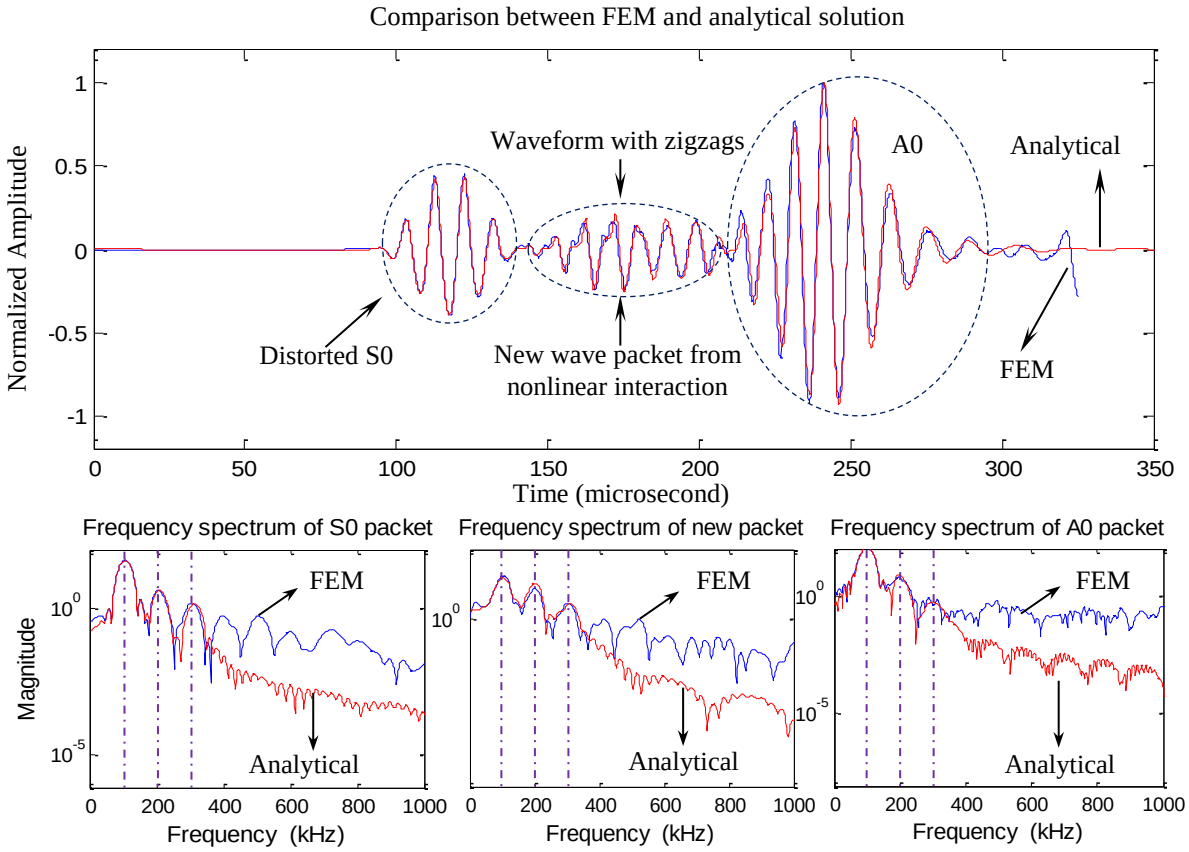

Figure 13: Comparison between FEM and analytical solution

5.3.3 Time-space wave filed and frequency-wavenumber representation

The **guided wave spatial propagation solver** in WaveFormRevealer was used to obtain the time-space domain wave field and frequency-wavenumber representation[13, 17] during this nonlinear interaction, as shown in Figure 14.

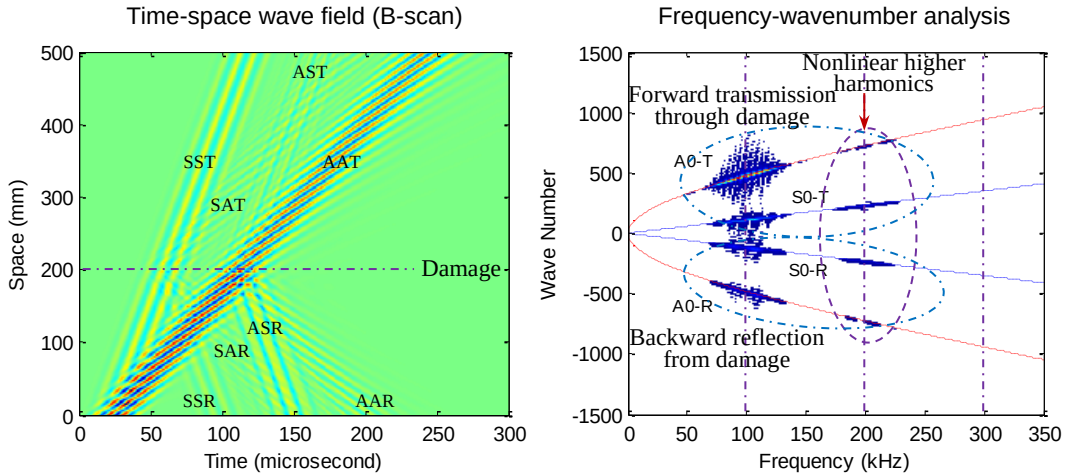

Figure 14: Time-space wave field and frequency-wavenumber analysis

The time-space wave field shows clearly the transmission, reflection and mode conversion phenomena. The frequency-wavenumber analysis shows the wave mode components and nonlinear higher harmonics. The spatial waveforms at 25, 50, 75, 100, 125 and 150microseconds are displayed in Figure 15. The spatial waveforms shows: (1) Lamb waves propagating into the structure at $T = 25\mu s$; (2) Lamb modes separating into distinct packets at $T = 50\mu s$; (3) Lamb wave packets interaction with the damage also at $T = 50\mu s$; (4) Wave transmission, reflection, mode conversion, nonlinear distortion of waveforms at various instances ($T = 75,100,125,150\mu s$).

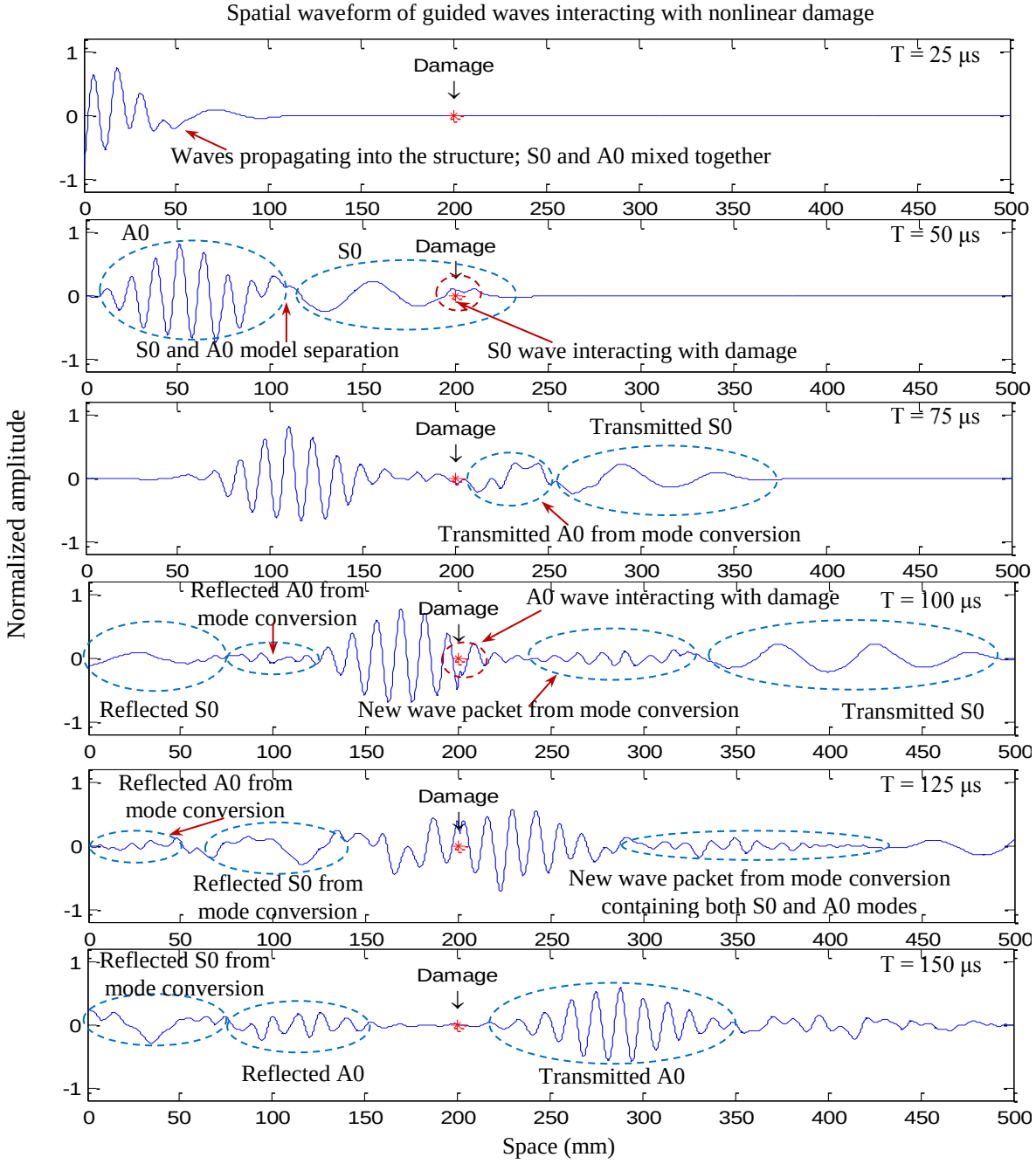

Figure 15: Analytical solution of guided wave spatial propagation and interaction with nonlinear damage

6. SUMMARY, CONCLUSIONS AND FUTURE WORK

6.1 Summary

This paper presented an analytical approach to modeling guided Lamb waves interacting with linear and nonlinear structural damage. The analytical model is constructed in frequency domain based on the exact solution for multi-mode guided waves excited by a PWAS. This analytical model considered four main aspects: (1) guided wave generation by T-PWAS (electrical to mechanical transduction); (2) Lamb wave multi-mode dispersive propagation in the host structure; (3) linear and nonlinear interaction between Lamb waves and damage; (4) guided wave detection by R-PWAS (mechanical to electrical transduction). The structural damage was modeled as a new wave source, where guided waves are transmitted, reflected, and mode-converted. In addition, when guided waves interact with nonlinear damage, both fundamental frequency and higher harmonics frequency components were present. Complex-number interaction coefficients were used to represent both magnitude and phase information of the interaction between Lamb waves and damage. Real time sensing signal at R-PWAS was obtained, as well as the time domain wave field of the interrogated structure and the frequency-wavenumber representation. A Graphical User Interface (GUI) called WaveFormRevealer (WFR) was developed based on this analytical model. Experiments and finite element simulations were conduct to verify the analytical model. It was found that the analytical procedure had good match with experiments and finite element simulations. Small differences were observed: they are due to the fact that we used 1-D straight crested wave theory.

6.2 Conclusions

The analytical model developed in this study could provide fast predictive solutions for multi-mode Lamb wave propagation and interaction with linear/nonlinear damage. The solutions compared well with experiments and finite element simulations. It was also found that computational time savings of several orders of magnitude are obtained by using the analytical model instead of FEM methods. WaveFormRevealer developed based on this analytical procedure allowed users to conduct fast parametric studies with their own designed materials, PWAS properties, specimen geometries, and excitations.

6.3 Future work

Rational methods of determining damage interaction coefficients values need to be found (not trial and error). Work should be carried out to extend the analysis to 2-D wave propagation (3-D FEM and 2-D WFR). This analytical simulation methodology should be extended to the study of wave propagation in composite structures with and without internal damage.

ACKNOWLEDGEMENTS

Support from Office of Naval Research # N00014-11-1-0271, Dr. Ignacio Perez, Technical Representative; Air Force Office of Scientific Research #FA9550-11-1-0133, Dr. David Stargel, Program Manager; are thankfully acknowledged.

REFERENCES

[1] J. L. Rose, [Ultrasonic Waves in Solid Media], Cambridge: Cambridge University Press (1999).

[2] K. F. Graff, [Wave motion in elastic solids], New York: Dover publications, INC.(1991).

[3] K. Y. Jhang, "Nonlinear Ultrasonic Techniques for Nondestructive Assessment of Micro Damage in Material: A Review," *International journal of Materials,* pp. 123-135 (2009).

[4] D. Dutta, H. Sohn and K. A. Harries, "A nonlinear acoustic technique for crack detection in metallic structures," *Structural Health Monitoring-an international journal,* pp. 573-573 (2009).

[5] F. Moser, L. J. Jacobs and J. Qu, "Modeling elastic wave propagation in waveguides with the finite element method," *NDT&E International,* pp. 225-234 (1999).

[6] M. Gresil, Y. Shen and V. Giurgiutiu, "Predictive modeling of ultrasonics SHM with PWAS transducers," in *8th International Workshop on Structural Health Monitoring*, Stanford, CA, USA (2011).

[7] V. Giurgiutiu, [Structural healthing monitoring with piezoelectric wafer active sensors], Elsevier Academic Press (2007).

[8] V. Giurgiutiu, "Tuned Lamb wave excitation and detection with piezoelectric wafer active sensors for structural health monitoring," *Journal of intelligent material systems and structures*, pp. 291-306 (2005).

[9] A. Raghavan and C. E. S. Cesnik, "Finite-dimensional piezoelectric transducer modeling for guided wave based structural health monitoring," *Smart Materials and Structures*, vol. 14, pp. 1448-1461 (2005).

[10] F.-K. Chang, ACELLENT, [Online]. Available: http://www.acellentsensors.com/.

[11] B. Lin, A. Kamal, V. Giurgiutiu and T. Kamas, "Multimodal Lamb Waves Power and Transer Function Analysis of Structurally-bounded PWAS," in *ASME 2012 Conference on Smart Materials, Adaptive Structures and Intelligent Systems*, Stone Mountain, Geogia, USA (2012).

[12] C. M. Yeum, H. Sohn and J. B. Ihn, "Lamb wave mode decomposition using concentric ring and circular PZT Transducers," *Wave Motion*, vol. 48, pp. 358-370 (2011).

[13] M. Ruzzene, "Frequency-wavenumber domain filtering for improved damage visualization," *Smart Materials and Structures*, vol. 16, pp. 2116-2129 (2007).

[14] J. H. Cantrell, "Nondestructive Evaluation of Metal Fatigue Using Nonlinear Acoustics," *CP1096 Review of Quantitative Nondestructive Evaluation*, pp. 19-32 (2009).

[15] Y. Shen and V. Giurgiutiu, "Predictive simulation of nonlinear ultrasonics," in *SPIE Smart Structures and Materials + Nondestructive Evalucation and Health Monitoring*, San Diego, California, USA (2012).

[16] Y. Shen and V. Giurgiutiu, "Simulation of interaction between Lamb waves and cracks for structural health monitoring with piezoelectric wafer active sensors," in *ASME 2012 Conference on Smart Materials, Adaptive Structures and Intelligent Systems*, Stone Moutain, Georgia, USA (2012).

[17] T. E. Michaels, J. E. Michaels and M. Ruzzene, "Frequency-wavenumber domain analysis of guided wavefeilds," *Ultrasonics*, vol. 51, pp. 452-466 (2011).